

# Computing A View Frustum To Maximize An Object's Image Area

Kok-Lim Low    Adrian Ilie

Department of Computer Science  
University of North Carolina at Chapel Hill  
Email: {lowk, adyilie}@cs.unc.edu

## ABSTRACT

This paper presents a method to compute a view frustum for a 3D object viewed from a given viewpoint, such that the object is completely enclosed in the frustum and the object's image area is also near-maximal in the given 2D rectangular viewing region. This optimization can be used to improve the resolution of shadow maps and texture maps for projective texture mapping. Instead of doing the optimization in 3D space to find a good view frustum, our method uses a 2D approach. The basic idea of our approach is as follows. First, from the given viewpoint, a conveniently-computed view frustum is used to project the 3D vertices of the object to their corresponding 2D image points. A tight 2D bounding quadrilateral is then computed to enclose these 2D image points. Next, considering the projective warp between the bounding quadrilateral and the rectangular viewing region, our method applies a technique of camera calibration to compute a new view frustum that generates an image that covers the viewing region as much as possible.

## 1 INTRODUCTION

In interactive computer graphics rendering, we often need to compute a view frustum from a given viewpoint such that a selected 3D object or a group of 3D objects is totally inside the rendered 2D rectangular image. This kind of view-frustum computation is usually needed when generating shadow maps [Williams78] from light sources, and images for projective texture mapping [Segal92, Hoff98].

The easiest way to compute such a view frustum is to pre-compute a simple 3D bounding volume, such as a bounding sphere, around the 3D object, and create a *symmetric* perspective view frustum that encloses the object's bounding volume. However, very often, this view frustum is not enclosing the 3D object tightly enough to produce an image of the object that covers the 2D rectangular viewing region as much as possible. We will refer to the 2D

rectangular viewing region as the *viewport*, and the projection of the 3D object in the viewport as the *object's image*. If the object's image is too small, we are not efficiently utilizing the available viewport area to produce a shadow map or projective texture map that could have higher-resolution due to a larger image of the object. A small image region of the object in a shadow map usually results in blocky shadow edges, and similarly, a low-resolution image region in a texture map can also result in a blocky rendered image.

Other methods increase the object's image area in the viewport by using a tighter 3D bounding volume, such as the 3D convex hull of the object [Berg97]. However, this is computationally expensive, and there is still a lot of room for improvement by manipulating the shape of the view frustum and the orientation of the image plane. Figure 1 shows an example.

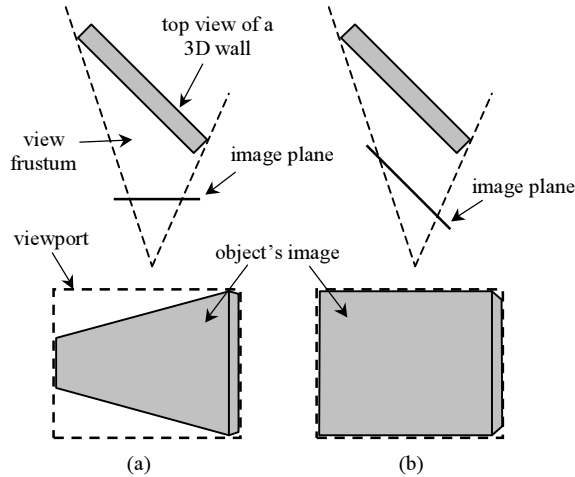


**Figure 1:** (a) The symmetric perspective view frustum cannot enclose the 3D object tightly enough, therefore, the object's image does not utilize efficiently the viewport area. (b) By manipulating the view frustum such that the image plane becomes parallel to the larger face of the 3D wall, we can improve the object's image to cover almost the whole viewport.

This paper presents a method to compute a view frustum for a 3D object viewed from a given viewpoint, such that the object's image is entirely inside the viewport and its area is also near-maximal. For computational efficiency,

our method does not seek to compute the optimal view frustum, but to compromise for one that is near-optimal. Instead of doing the optimization in 3D space to find a good view frustum, our method uses a 2D approach. This makes the method more efficient and simpler to implement.

## 2 OVERVIEW OF METHOD

Without loss of generality, we will describe our method in the context of the OpenGL API [Woo99]. In OpenGL, defining a view frustum from an arbitrary viewpoint requires the definition of two transformations: the *view transformation*, which transforms points in the world coordinate system into the eye coordinate system; and the *projection transformation*, which transforms points in the eye coordinate system into the normalized device coordinate (NDC) system.

Given a viewpoint, a 3D object in the world coordinate system, and the viewport's width and height, our objective is to compute a valid view frustum (i.e. a view transformation and a projection transformation) that maximizes the area of the object's image in the viewport. We provide an overview of our method below and the key steps are described in more detail in Sections 3 and 4.

### *Start with an initial frustum*

We start with a conveniently-computed view frustum by bounding the object with a sphere and then creating a symmetric perspective view frustum that encloses the sphere. The view transformation and the projection transformation that represent this frustum can be readily obtained using the OpenGL commands `glGetDoublev(GL_MODELVIEW_MATRIX, m)` and `glGetDoublev(GL_PROJECTION_MATRIX, p)`, respectively.

We use the two transformations and the viewport settings to explicitly transform all the 3D vertices of the object from the world coordinates to their corresponding 2D image points.

### *Compute tight bounding quadrilateral (Section 3)*

We compute a tight bounding quadrilateral of the 2D image points. The basic idea, illustrated in Figure 2, is to start by computing a 2D convex hull of the image points, and then incrementally removing the edges of the convex hull until a bounding quadrilateral remains.

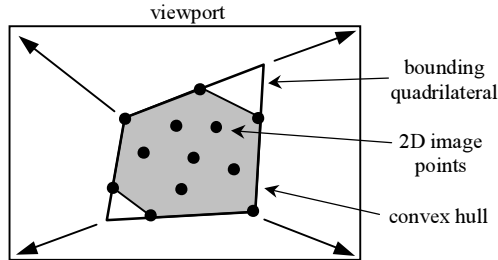


**Figure 2:** The 3D vertices of the object are first projected onto their corresponding 2D image points. A 2D convex hull is computed for these image points, and it is then incrementally reduced to a quadrilateral. The bounding quadrilateral is related to the viewport’s rectangle by a projective warp. This warping effect can be achieved by rotating and moving the image plane.

*Compute optimized view frustum (Section 4)*

The most important idea of our method lies in the observation that the bounding quadrilateral and the rectangular viewport are related only by a projective warp or 2D collineation (see Chapter 2 of [Faugeras93]). Equally important to know is that this projective warp from the bounding quadrilateral to a rectangle can be achieved by merely rotating and moving the image plane.

**3 COMPUTING TIGHT BOUNDING QUADRILATERAL**

We start by computing the 2D convex hull of the 2D image points, using methods such as Graham’s algorithm [O’Rourke98]. The time complexity of this step is  $O(m \log m)$ , where  $m$  is the number of image points.

Aggarwal et al. presented a general technique to compute the smallest convex  $k$ -sided polygon to enclose a given convex  $n$ -sided polygon [Aggarwal85]. Their method runs in  $O(n^2 \log n \log k)$  time, however, and can be difficult to implement.

Here, we describe an alternative algorithm to compute a convex bounding quadrilateral. Our algorithm produces only near-optimal results, but is simple to implement and has time complexity  $O(n \log n)$ .

Our algorithm obtains the convex bounding quadrilateral by iteratively removing edges from the convex hull using a greedy approach until only four

edges remain. To remove an edge  $i$ , we need to first make sure that the sum of the interior angles it makes with the two adjacent edges is more than  $180^\circ$ . Then, we extend the two adjacent edges towards each other to intersect at a point (see Figure 3).

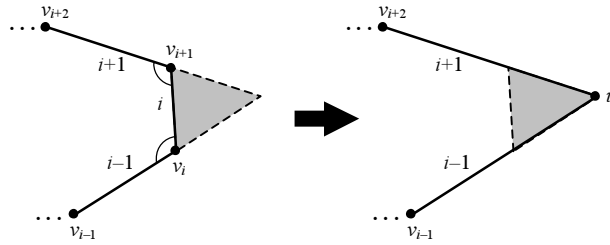


**Figure 3:** Removing edge  $i$ .

For a convex hull with  $n$  edges, we iterate  $n - 4$  times, removing one edge each time to yield a quadrilateral. At each iteration, we choose to remove the edge whose removal would add the smallest area to the resulting polygon. For example, in Figure 3, removing edge  $i$  adds the gray-shaded area to the resulting polygon. We use a heap to find the edge to remove in constant time. After the edge is removed, we must update the area values of its two adjacent edges. Since initially building the heap requires  $O(n \log n)$  time, and each iteration has two  $O(\log n)$  heap updates, the time complexity of our algorithm is  $O(n \log n)$ .

It can be easily proved that for any convex polygon of five or more sides, there always exists at least one edge that can be removed. Since the resulting polygon is also a convex polygon, by induction, we can always reduce the initial input convex hull to a convex quadrilateral.

Of course, if the initial convex hull is already a quadrilateral, we do not need to do anything. If the initial convex hull is a triangle, we just create a bounding parallelogram whose diagonal corresponds to the longest edge of the triangle, and three of its corners coincide with the three corners of the triangle. This ensures that the object's image occupies half the viewport, which is the optimal area in this case.

## 4 COMPUTING OPTIMIZED VIEW FRUSTUM

After we have found a tight bounding quadrilateral, we want to compute a view frustum that warps the quadrilateral to the viewport's rectangle as illustrated in Figure 2.

First, we need to decide to which corner of the viewport's rectangle each quadrilateral corner is to be warped. We have chosen to match the longest edge and its opposite edge of the quadrilateral with the longer edges of the viewport's rectangle.

Using the view transformation and the projection transformation of the conveniently-computed view frustum, we inverse-project each corner of the bounding quadrilateral back into the 3D world coordinate system as a ray originating from the viewpoint. Taking the world coordinates of any 3D point on the ray and pairing it with the 2D *pixel coordinates* of the corresponding corner of the viewport's rectangle, we get a *pair-correspondence*. With four pair-correspondences, one for each corner, we are able to use a camera calibration technique to solve for the desired view frustum.

### 4.1 A Camera Calibration Technique

For a pinhole camera, which is the camera model used in OpenGL, the effect of transforming a 3D point in the world coordinate system into a 2D image point in the viewport can be described by the following expression:

$$\begin{pmatrix} u_i \\ v_i \\ w_i \end{pmatrix} = \mathbf{P} \cdot \begin{pmatrix} X_i \\ Y_i \\ Z_i \\ 1 \end{pmatrix} = \begin{pmatrix} a & 0 & c_x \\ 0 & b & c_y \\ 0 & 0 & 1 \end{pmatrix} \cdot \begin{pmatrix} r_{11} & r_{12} & r_{13} & t_1 \\ r_{21} & r_{22} & r_{23} & t_2 \\ r_{31} & r_{32} & r_{33} & t_3 \end{pmatrix} \cdot \begin{pmatrix} X_i \\ Y_i \\ Z_i \\ 1 \end{pmatrix} \quad (1)$$

where

- $a$ ,  $b$ ,  $c_x$  and  $c_y$  are collectively called the *intrinsic parameters* of the camera,
- $r_{ij}$  and  $t_i$  respectively define the *rotation* and *translation* of the view transformation, and they are called the *extrinsic parameters* of the camera,
- $(X_i, Y_i, Z_i, 1)^T$  are the homogeneous coordinates of a point in the world coordinate system, and
- the pixel coordinates of the 2D image point are

$$\begin{pmatrix} x_i \\ y_i \end{pmatrix} = \begin{pmatrix} u_i/w_i \\ v_i/w_i \end{pmatrix}. \quad (2)$$

$\mathbf{P}$  is a  $3 \times 4$  projection matrix. Note that this is not the same as OpenGL's projection transformation:  $\mathbf{P}$  maps a 3D point in the world coordinate system to 2D pixel coordinates, whereas OpenGL's projection transformation maps a 3D point in the eye coordinate system to a 3D point in the NDC. (Later on we will describe how to construct OpenGL's projection matrix from  $\mathbf{P}$ .)

Since the viewpoint's position is known, we can first apply a translation to the world coordinate system such that the viewpoint is now located at the origin. We will refer to this as the *shifted world coordinate system*, and with it, we can simplify (1) to

$$\begin{pmatrix} u_i \\ v_i \\ w_i \end{pmatrix} = \mathbf{P} \cdot \begin{pmatrix} X_i \\ Y_i \\ Z_i \end{pmatrix} = \begin{pmatrix} a & 0 & c_x \\ 0 & b & c_y \\ 0 & 0 & 1 \end{pmatrix} \cdot \begin{pmatrix} r_{11} & r_{12} & r_{13} \\ r_{21} & r_{22} & r_{23} \\ r_{31} & r_{32} & r_{33} \end{pmatrix} \cdot \begin{pmatrix} X_i \\ Y_i \\ Z_i \end{pmatrix} \quad (3)$$

where  $\mathbf{P}$  is now a  $3 \times 3$  matrix, and  $(X_i, Y_i, Z_i)^T$  are the 3D coordinates of a point in the shifted world coordinate system.

To solve for the intrinsic and extrinsic camera parameters, we will first solve for the matrix  $\mathbf{P}$ , and then decompose  $\mathbf{P}$  into the individual camera parameters.

#### 4.1.1 Solving for the Projection Matrix

If we write  $\mathbf{P}$  as

$$\mathbf{P} = \begin{pmatrix} p_{11} & p_{12} & p_{13} \\ p_{21} & p_{22} & p_{23} \\ p_{31} & p_{32} & p_{33} \end{pmatrix} \quad (4)$$

then the pixel coordinates of the  $i$ th 2D image point can be written as

$$\begin{aligned} x_i &= \frac{u_i}{w_i} = \frac{p_{11}X_i + p_{12}Y_i + p_{13}Z_i}{p_{31}X_i + p_{32}Y_i + p_{33}Z_i} \\ y_i &= \frac{v_i}{w_i} = \frac{p_{21}X_i + p_{22}Y_i + p_{23}Z_i}{p_{31}X_i + p_{32}Y_i + p_{33}Z_i}. \end{aligned} \quad (5)$$

We can rearrange (5) to get

$$\begin{aligned}
p_{11}X_i + p_{12}Y_i + p_{13}Z_i - x_i(p_{31}X_i + p_{32}Y_i + p_{33}Z_i) &= 0 \\
p_{21}X_i + p_{22}Y_i + p_{23}Z_i - y_i(p_{31}X_i + p_{32}Y_i + p_{33}Z_i) &= 0.
\end{aligned} \tag{6}$$

Because of the divisions  $u_i/w_i$  and  $v_i/w_i$  in (5),  $\mathbf{P}$  is defined up to an arbitrary scale factor, and has only eight independent entries. Therefore, the four pair-correspondences we have previously obtained are sufficient to solve for  $\mathbf{P}$ . Note that because of the removal of the translation in (3), the 3D point in each pair-correspondence must now be translated into the shifted world coordinate system. Note that by construction, our bounding quadrilateral is strictly convex, so no three corners will be collinear and we do not need to worry about degeneracy.

With the four pair-correspondences, we can form a homogeneous linear system

$$\mathbf{A} \cdot \mathbf{p} = \mathbf{0} \tag{7}$$

where

$$\mathbf{p} = (p_{11}, p_{12}, p_{13}, p_{21}, p_{22}, p_{23}, p_{31}, p_{32}, p_{33})^T \tag{8}$$

and

$$\mathbf{A} = \begin{pmatrix} X_1 & Y_1 & Z_1 & 0 & 0 & 0 & -x_1X_1 & -x_1Y_1 & -x_1Z_1 \\ 0 & 0 & 0 & X_1 & Y_1 & Z_1 & -y_1X_1 & -y_1Y_1 & -y_1Z_1 \\ X_2 & Y_2 & Z_2 & 0 & 0 & 0 & -x_2X_2 & -x_2Y_2 & -x_2Z_2 \\ 0 & 0 & 0 & X_2 & Y_2 & Z_2 & -y_2X_2 & -y_2Y_2 & -y_2Z_2 \\ X_3 & Y_3 & Z_3 & 0 & 0 & 0 & -x_3X_3 & -x_3Y_3 & -x_3Z_3 \\ 0 & 0 & 0 & X_3 & Y_3 & Z_3 & -y_3X_3 & -y_3Y_3 & -y_3Z_3 \\ X_4 & Y_4 & Z_4 & 0 & 0 & 0 & -x_4X_4 & -x_4Y_4 & -x_4Z_4 \\ 0 & 0 & 0 & X_4 & Y_4 & Z_4 & -y_4X_4 & -y_4Y_4 & -y_4Z_4 \end{pmatrix} \tag{9}$$

For the homogeneous system  $\mathbf{A} \cdot \mathbf{p} = \mathbf{0}$ , the vector  $\mathbf{p}$  can be computed using SVD (singular value decomposition) related techniques as the eigenvector corresponding to the only zero eigenvalue of  $\mathbf{A}^T \mathbf{A}$ . In other words, if the SVD of  $\mathbf{A}$  is  $\mathbf{U} \mathbf{D} \mathbf{V}^T$ , then  $\mathbf{p}$  is the column of  $\mathbf{V}$  corresponding to the only zero singular value of  $\mathbf{A}$ . For more details about camera calibration, see [Trucco98], and for a comprehensive introduction to linear algebra and SVD, see [Strang88]. An implementation of SVD can be found in [Press93].



#### 4.1.2 Computing Camera Parameters

From the computed projection matrix  $\mathbf{P}$ , we want to express the intrinsic and extrinsic parameters as closed-form functions of the matrix entries. Recall that the computed matrix is defined only up to an arbitrary scale factor, therefore, to use the relationship

$$\mathbf{P} = \begin{pmatrix} ar_{11} + c_x r_{31} & ar_{12} + c_x r_{32} & ar_{13} + c_x r_{33} \\ br_{21} + c_y r_{31} & br_{22} + c_y r_{32} & br_{23} + c_y r_{33} \\ r_{31} & r_{32} & r_{33} \end{pmatrix}, \quad (10)$$

we must first properly normalize  $\mathbf{P}$ . We observe that the last row in the matrix above correspond to the last row of the rotation matrix, which must be of unit length. So we normalize  $\mathbf{P}$  by dividing it by  $\pm\sqrt{p_{31}^2 + p_{32}^2 + p_{33}^2}$ , with the choice of sign still arbitrary.

We can now extract the camera parameters. For clarity, we write the three rows of  $\mathbf{P}$  as the following column vectors:

$$\begin{aligned} \mathbf{p}_1 &= (p_{11}, p_{12}, p_{13})^\top, \\ \mathbf{p}_2 &= (p_{21}, p_{22}, p_{23})^\top, \\ \mathbf{p}_3 &= (p_{31}, p_{32}, p_{33})^\top. \end{aligned} \quad (11)$$

The values of the parameters can be computed as follows:

$$\begin{aligned} c_x &= \mathbf{p}_1^\top \mathbf{p}_3, \\ c_y &= \mathbf{p}_2^\top \mathbf{p}_3, \\ a &= -\sqrt{\mathbf{p}_1^\top \mathbf{p}_1 - c_x^2}, \\ b &= -\sqrt{\mathbf{p}_2^\top \mathbf{p}_2 - c_y^2}, \\ (r_{11}, r_{12}, r_{13})^\top &= (\mathbf{p}_1 - c_x \mathbf{p}_3)/a, \\ (r_{21}, r_{22}, r_{23})^\top &= (\mathbf{p}_2 - c_y \mathbf{p}_3)/b, \\ (r_{31}, r_{32}, r_{33})^\top &= \mathbf{p}_3. \end{aligned} \quad (12)$$

The sign of the normalization affects only the values of  $r_{ij}$ . It can be determined as follows. First, we use the rotation matrix  $[r_{ij}]$  computed in the above procedure to transform the 4 shifted world points in the pair-correspondences. Since these 3D points are all in front of the camera, their

transformed  $z$ -coordinates should be negative, because the camera is looking in the  $-z$  direction in the eye coordinate system. If it is not the case, we correct the  $r_{ij}$  by changing their signs.

#### 4.1.3 Conversion to OpenGL Matrices

From the camera parameters obtained above, the OpenGL view transformation matrix is

$$\mathbf{M}_{\text{MODELVIEW}} = \begin{pmatrix} r_{11} & r_{12} & r_{13} & (-r_{11}v_x - r_{12}v_y - r_{13}v_z) \\ r_{21} & r_{22} & r_{23} & (-r_{21}v_x - r_{22}v_y - r_{23}v_z) \\ r_{31} & r_{32} & r_{33} & (-r_{31}v_x - r_{32}v_y - r_{33}v_z) \\ 0 & 0 & 0 & 1 \end{pmatrix}, \quad (13)$$

where  $(v_x, v_y, v_z)^T$  is the position of the viewpoint in the world coordinate system.

The OpenGL projection matrix is

$$\mathbf{M}_{\text{PROJECTION}} = \begin{pmatrix} \frac{-2a}{W} & 0 & 1 - \frac{2c_x}{W} & 0 \\ 0 & \frac{-2b}{H} & 1 - \frac{2c_y}{H} & 0 \\ 0 & 0 & \frac{-(f+n)}{f-n} & \frac{-2fn}{f-n} \\ 0 & 0 & -1 & 0 \end{pmatrix}, \quad (14)$$

where  $W$  and  $H$  are the width and height of the viewport in pixels, respectively, and  $n$  and  $f$  are the distances of the near and far plane from the viewpoint, respectively. If  $n$  and  $f$  cannot be known beforehand, a simple and efficient way to compute good values for  $n$  and  $f$  is to transform the bounding sphere of the 3D object into the eye coordinate system and compute

$$\begin{aligned} n &= -o_z - r, \\ f &= -o_z + r, \end{aligned} \quad (15)$$

where  $o_z$  is the  $z$ -coordinate of the center of the sphere in the eye coordinate system, and  $r$  is the radius of the sphere.

## 5 EXAMPLES

In Figure 4, we show three example results. The images in the leftmost column were generated using symmetric perspective view frusta enclosing the bounding spheres of the respective objects. The middle column shows the bounding quadrilaterals computed using our algorithm described in Section 3. The rightmost column shows the images generated using the new frusta computed using our method. Note that each object is always viewed from the same viewpoint for both the unoptimized and optimized view frusta.

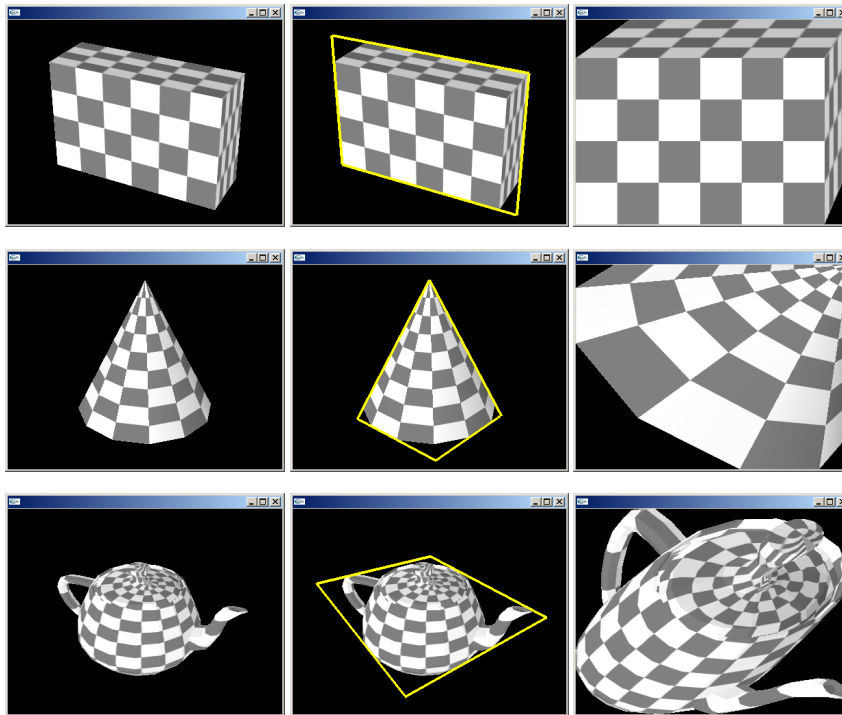


Figure 4: Example results.

## 6 DISCUSSION

If the viewpoint is dynamic, a new view frustum has to be computed for every rendered frame. In the computation of the 2D convex hull and the bounding

quadrilateral, if the number of 2D image points is too large, it may be difficult to render at interactive rates. For a non-deformable 3D object, we can first pre-compute its 3D convex hull, and project only the 3D vertices of the convex hull onto the viewport as 2D image points. This will reduce the number of 2D points that our algorithm needs to work with. If the 3D convex hull is still too complex, we can simplify it by reducing its number of faces and vertices. Note that the simplified hull should totally contain the original convex hull. The 3D convex hull and its simplified version would be computed in a pre-processing step.

Besides the advantage of increasing the resolution of the object's image, our method can also improve the temporal consistency of the object's image resolution from frame to frame. If the 3D object has a predominantly large face (or a predominant silhouette), the image plane of the computed view frustum will tend to be oriented with it for many viewpoints. This results in a more stable image plane, and therefore more consistent object's image resolution. This benefit is important to projector-based displays in which projective texture mapping is used to produce perspective-correct imagery for the tracked users [Raskar98]. In this application, texture maps are generated from the user's viewpoint, and are then texture-mapped onto the display surfaces using projective texture mapping. Excessive changes in texture map resolution when the viewpoint moves can cause undesired effects in the projected imagery.

Something we wish we had done is to prove how much worse our approximated smallest enclosing quadrilaterals are, compared to the truly optimal ones. Such a proof would most likely be nontrivial. Since we also did not have an implementation of the algorithm described in [Aggarwal85] available to us, we could not do any empirical comparisons between our approximations and the true minimum areas. However, from manual inspection of our results, our algorithm always produced results that are within our expectation of being good approximations of the smallest possible quadrilaterals. Note that even if the quadrilateral is the smallest possible, it still cannot guarantee that the object's image area will be the largest possible. This is because the projective warp does not "scale" every part of the quadrilateral uniformly.

Raskar described a method to append a matrix that represents a 2D collineation to an OpenGL projection matrix to achieve the desired projective warp of the original image [Raskar99]. Though such a 2D projective warp preserves collinearity in the 2D image plane, it does not preserve collinearity in the 3D NDC. This results in incorrect depth interpolation, and therefore,

incorrect interpolation of surface attributes. Our method can also be used for oblique projector rendering on planar surfaces. In this case, we need to compute the view frustum that warps the rectangular viewport to a smaller quadrilateral inside the viewport. The results from our method do not have the incorrect depth interpolation problem.

## ACKNOWLEDGEMENTS

We wish to thank Jack Snoeyink for referring us to the previous work on minimal enclosing polygons, as well as to Anselmo Lastra and Greg Welch for their many useful suggestions.

Support for this research comes from NSF ITR grant “Electronic Books for the Tele-immersion Age” and NSF Cooperative Agreement no. ASC-8920219: “NSF Science and Technology Center for Computer Graphics and Scientific Visualization.”

## REFERENCES

- [Aggarwal85] Alok Aggarwal, J. S. Chang, Chee K. Yap. *Minimum Area Circumscribing Polygons*. The Visual Computer: International Journal of Graphics, 1:112–117, 1985.
- [Faugeras93] Olivier Faugeras. *Three-Dimensional Computer Vision*. MIT Press, 1993.
- [Foley90] James D. Foley, Andries van Dam, Steven K. Feiner and John F. Hughes. *Computer Graphics: Principles and Practice, Second Edition*. Addison Wesley, 1990.
- [Hoff98] Kenneth E. Hoff. *Understanding Projective Textures*. <http://www.cs.unc.edu/~hoff/techrep/projtextures.html>, 1998.
- [O’Rourke98] Joseph O’Rourke. *Computational Geometry in C, Second Edition*. Cambridge University Press, 1998.
- [Press93] William H. Press, Saul A. Teukolsky, William T. Vetterling, Brian P. Flannery. *Numerical Recipes in C: The Art of Scientific Computing, Second Edition*. Cambridge University Press, January 1993.

- [Raskar98] Ramesh Raskar, Matt Cutts, Greg Welch, Wolfgang Stuerzlinger. *Efficient Image Generation for Multiprojector and Multisurface Display Surfaces*. Rendering Techniques '98, proceedings of the 9th Eurographics Workshop on Rendering, June 1998.
- [Raskar99] Ramesh Raskar. *Oblique Projector Rendering on Planar Surfaces for a Tracked User*. SIGGRAPH Sketch, 1999. <http://www.cs.unc.edu/~raskar/Oblique/oblique.pdf>
- [Segal92] Mark Segal, Carl Korobkin, Rolf van Widenfelt, Jim Foran, Paul E. Haeberli. *Fast Shadows and Lighting Effects Using Texture Mapping*. SIGGRAPH 92 Conference Proceedings, Annual Conference Series, ACM SIGGRAPH, Addison Wesley, vol. 26, pp. 249–252, July 1992.
- [Strang88] Gilbert Strang. *Linear Algebra and Its Applications, Third Edition* (1988). International Thomson Publishing.
- [Trucco98] Emanuele Trucco and Alessandro Verri. *Introductory Techniques for 3-D Computer Vision*. Prentice Hall, 1998.
- [Williams78] Lance Williams. *Casting Curved Shadows on Curved Surfaces*. Proceedings of SIGGRAPH 78. In *Computer Graphics*, 12(3):270–274, ACM SIGGRAPH, August 1978.
- [Woo99] Mason Woo, Jackie Neider, Tom Davis, Dave Shreiner (OpenGL Architecture Review Board). *OpenGL Programming Guide, Third Edition: The Official Guide to Learning OpenGL, Version 1.2*. Addison Wesley, 1999.